Influence of the inclination of columnar defects on the reversible magnetization of high-T_c superconductors

V. Hardy, S. Hébert, M. Hervieu, Ch. Simon, and J. Provost
Laboratoire CRISMAT, UMR 6508, ISMRA et Université de Caen, 6 Bd du Maréchal Juin, 14050 Caen-Cedex, France

A. Wahl and A. Ruyter
Laboratoire LEMA, Université F. Rabelais, Parc de Grandmont, 37200 Tours, France

(Received 1 July 1998)

Reversible magnetization has been studied in crystals of highly anisotropic high-T_c superconductors, containing columnar defects oriented either along the c axis or at an angle θ_i from it. With the magnetic field applied along c, a similar dip in the M-vs-ln(B) curves is observed for both track orientations. The location of this dip is shown to be related to B_{cd}, the field at which the vortex and track densities per ab plane are the same. The vortex pinning energy, extracted from the low field regime, is found to be slightly larger for $\theta_i = 60°$ than for $\theta_i = 0°$. This effect is ascribed to the larger size of the track projections on the ab planes, in the case of inclined tracks. On the basis of the random nature of the track distribution, a model is proposed to account for the smooth character of the crossover between the low field ($B \ll B_{cd}$) and high field ($B \gg B_{cd}$) regimes. [S0163-1829(98)04146-0]

I. INTRODUCTION

Columnar defects (CDs), introduced in superconducting cuprates by heavy-ion irradiation, strongly modify the vortex pinning ability. This modification affects not only irreversible properties such as the critical current densities, but also the reversible magnetization $M_{\rm rev}$. When the magnetic field and the CDs are aligned along the c axis, the $M_{\rm rev}$-vs-ln(B) curves exhibit[1–3] an unusual ''dip'' around the fluence equivalent field $B_{\Phi t} = \Phi t \times \Phi_0$ (Φt being the ion fluence). This behavior was related to the reduced line energy of a vortex located in a track. On the basis of the London model, estimates of the pinning energy were extracted[2,3] from the low field regime ($B \ll B_{\Phi t}$).

Up to now, these studies of reversible magnetization in irradiated samples were carried out with both the magnetic field and the set of CDs parallel to the c axis. In the present paper, we report measurements of $M_{\rm rev}$, still with $B \| c$, but for CDs inclined by an angle θ_i from the c axis. This study was performed on crystals of $Bi_2Sr_2CaCu_2O_8$ (Bi-2212) and $Tl_2Ba_2CaCu_2O_8$ (Tl-2212). In such very anisotropic superconductors, the weak vortex correlation perpendicular to the ab planes can give rise to original states of the vortex matter. One can get information about such vortex states by varying the orientations of the field and of the CDs, with respect to the c axis.[4] For instance, with the field applied along c in a sample containing inclined CDs, very different magnetic responses are expected depending on whether one deals with stiff line vortices or completly decoupled pancakes.

The first goal of the present work is to investigate, in the case of inclined CDs, the persistence or not of the dip in $M_{\rm rev}$-vs-ln(B). In a second step, we compare the pinning energies in samples with tracks either parallel to the c axis or tilted from it. Indeed, the track projections on the ab planes are larger in the latter case, and this should affect the electromagnetic contribution to vortex pinning in very anisotropic superconductors. The aim of the last part of this paper is to determine how far the whole shape of $M_{\rm rev}$-vs-ln(B) curves can be accounted for by the random nature of the track distribution.

The paper is organized as follows. In Sec. II, some experimental details are given about the samples, the irradiation, and the measuring procedure. Section III reports series of $M_{\rm rev}$-vs-ln(B) curves for CDs inclined at $\theta_i = 45°$ in Bi-2212, or inclined at $\theta_i = 60°$ in Tl-2212. In both compounds, the results are compared with those of CDs at $\theta_i = 0°$. Section IV reports the extraction of pinning energies in Tl-2212, for $\theta_i = 0°$ and $\theta_i = 60°$. In Sec. V, a model is proposed to account for the shifting of $M_{\rm rev}$-vs-ln(B) curves between the virgin and irradiated states. This model includes a renormalization of the penetration depth due to screening effects, and takes into account the random character of the track distribution. Fitting curves are compared to those derived from the model proposed by Bulaevskii *et al.*[5] Section VI points out the main results and their implications.

II. EXPERIMENTAL

A. Sample preparation

Single crystals of $Bi_2Sr_2CaCu_2O_8$ (Bi-2212) and $Tl_2Ba_2CaCu_2O_8$ (Tl-2212) have been grown following methods described in Refs. 6 and 7, respectively. For both compounds, the as-synthesized samples are slightly overdoped. The T_c's before irradiation are equal to 83 K and 104 K, for Bi-2212 and Tl-2212, respectively.

B. Irradiation procedure

The crystals were irradiated at room temperature with 6-GeV Pb ions at the accelerator GANIL (Caen, France). These ions are known to induce, in both compounds, the creation of continuous, amorphous tracks, with a core radius

TABLE I. Label and main characteristics of the four studied crystals.

Denomination	Compound	Fluence (cm^{-2})	Irradiation angle	Dimensions (μm^3)
Bi00	Bi-2212	10^{11}	0°	$\sim 1460\times 880\times 20$
Bi45	Bi-2212	10^{11}	45°	$\sim 1190\times 750\times 20$
Tl00	Tl-2212	5×10^{10}	0°	$930\times 610\times 80$
Tl60	Tl-2212	5×10^{10}	60°	$650\times 460\times 30$

around $4.5-5$ nm.[8,9] Two kinds of irradiation were carried out: the ion-beam was oriented either parallel or at θ_i to the c axis. In both configurations, the ion fluence Φt was the same. For Bi-2212, $\Phi t = 10^{11}$ cm^{-2} and $\theta_i = 45°$, while for Tl-2212, $\Phi t = 5\times 10^{10}$ cm^{-2} and $\theta_i = 60°$. This study essentially involves four samples, whose characteristics are collected in Table I.

Measurements of reversible magnetization need samples of large volume, but the irradiation imposes limits in thickness. Indeed, the ion path in the target must be much lower than the projected range, in order to ensure an homogeneous damage across the entire sample thickness. The projected range of 6-GeV Pb ions in Bi-2212 and Tl-2212 is about 150 μm. It must also be taken into account that a beam inclination increases the effective ion path by a factor $(1/\cos\theta_i)$.

C. Measuring procedure

The measurements were performed by means of a superconducting quantum interference device (SQUID) magnetometer, with the external magnetic field H applied along the c axis. The samples were mounted on a copper rod, of length and diameter equal to 220 and 1 mm, respectively. The bottom extremity of the rod was shaped into a ring to ensure a good radial centering of the sample. The crystals were directly glued on the rod with a small amount of silicon vacuum grease. This sample mounting yields a well-shaped SQUID response at $T > T_c$, which is required to reliably substract the background signal.

Reversible magnetization was measured as a function of H. At fixed T, the magnetic field was first increased from a value H_{min}, lower than the irreversible field, up to $H_{max} = 5$ T, and then it was decreased from H_{max} down to H_{min}. In order to minimize the problems steming from field stabilization and drift in the SQUID detector, a waiting time of 5 mn was respected after each field change, and the three first measuring scans after this pause were rejected. The magnetic moment was then obtained by averaging 20 scans of length 3 cm. The temperature stability was held at 0.2%.

Curves were registered at various temperatures, including one much higher than T_c in order to measure the background signal resulting from both the sample holder and the normal state response of the sample. This background signal is nearly T independent for $T > T_c$. It was measured at 120 K for Bi-2212, and at 130 K for Tl-2212. The moment values at these temperatures are rather small (for instance, lower than 5×10^{-6} emu around 1 T), but they cannot be neglected. The reversible magnetization curves presented below have thus been corrected by substracting this field dependent background signal.

Owing to the great pinning efficiency of CDs, the reversible field range rapidly shrinks as T decreases, and impedes the access to the low field regime where M_{rev}-vs-ln(B) exhibits a positive slope. As done in a previous study,[10] we used the irreversible values on the increasing and decreasing branches (denoted M_+ and M_-, respectively), to evaluate the equilibrium magnetization $M_{rev} \simeq (M_+ + M_-)/2$. In the virgin state, such a procedure yields data in very good agreement with an extrapolation of the high field regime following the London model. In irradiated samples, this method yields a M_{rev}-vs-ln(B) curve which appears, close to the irreversibility point, as a smooth extrapolation of the *true* reversible magnetization, but which suddenly becomes very noisy below a field value, i.e., when the irreversible part of the magnetization becomes much larger than the reversible part. This T-dependent field value limits the range where M_{rev} is evaluated from M_+ and M_-.

III. EQUILIBRIUM MAGNETIZATION IN MISALIGNED CONFIGURATIONS

The previous works[1–3] about M_{rev} in presence of CDs were carried out in an ''aligned'' configuration: $\mathbf{B}\|\mathbf{c}\|$CDs. Figures 1 and 2 show M_{rev}-vs-ln(B) curves in Bi45 and Tl60, i.e., (see Table I), for $\mathbf{B}\|\mathbf{c}$ and CDs at θ_i to the c axis. In both samples, the M_{rev}-vs-ln(B) curves exhibit a clear dip at intermediate fields. Similar unusual field dependencies of M_{rev} have been also observed in Bi00 and Tl00 (aligned configurations), in qualitative accordance with the literature.[1–3] However, for the misaligned configurations, the dip is not

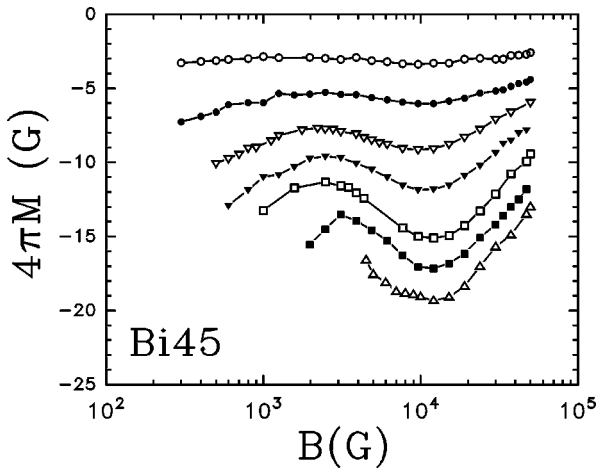

FIG. 1. Curves of reversible magnetization versus field, for a Bi-2212 crystal irradiated by 10^{11} Pb cm^{-2} at an angle $\theta_i = 45°$ from c. The temperatures are (from bottom to top): 50, 55, 60, 65, 70, 75, 78 K.

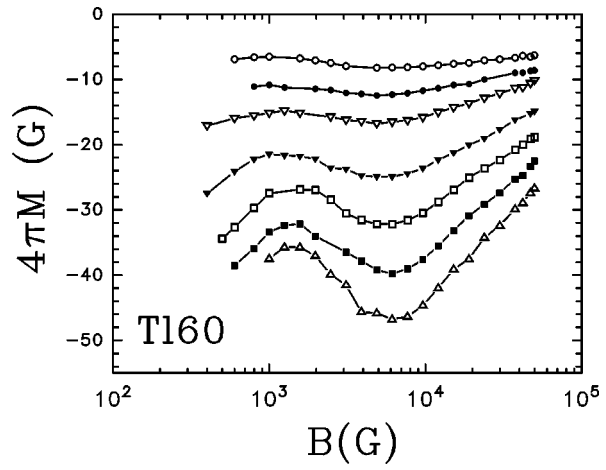

FIG. 2. Curves of reversible magnetization versus field, for a Tl-2212 crystal irradiated by 5×10^{10} Pb cm^{-2} at an angle $\theta_i=60°$ from c. The temperatures are (from bottom to top): 70, 75, 80, 85, 90, 92.5, 95 K.

centered around $B_{\Phi t}$, as it is the case for $\theta_i=0°$. The $B_{\Phi t}$ of Bi45 and Tl60 are 2 T and 1 T, respectively. Actually, one observes in Figs. 1 and 2 that the dip rather takes place around the ''perpendicular equivalent field,'' $B_{cd}=B_{\Phi t}\times\cos(\theta_i)$, which is equal to 1.41 and 0.5 T, for Bi45 and Tl60, respectively.

This relationship between B_{cd} and the location of the dip is pointed out in Fig. 3. At a given temperature for each compound, reversible magnetization curves of the samples at $\theta_i=0°$ and $\theta_i\neq0°$ are plotted versus B/B_{cd}. In both compounds, one observes that the dips for $\theta_i=0°$ and $\theta_i\neq0°$ take place at the same value of B/B_{cd}. This value is close to 1, but may be slightly different, as in Figs. 3(a) and 3(b). It was previously reported[1,2] that there is not a systematic, perfect correspondence between the dip location and the matching field. In particular, there is always a noticeable shifting of the dip towards lower fields as T increases.

The characteristic field B_{cd} is directly connected to n_{cd}, the track density in each ab plane:

$$B_{cd}=n_{cd}\times\Phi_0. \tag{3.1}$$

The existence of a close relationship between the dip location and n_{cd} demonstrates that the vortices in our misaligned configurations do not behave as stiff lines oriented along H. Rather, such a role of n_{cd} is consistent with a regime where pancake vortices can accommodate to the track projections in each ab plane. Such a behavior does not necessarily imply a complete vortex decoupling. The degree of pancake correlation along the track direction is not easy to investigate experimentally. In aligned configurations ($\mathbf{B}\|\mathbf{c}\|$CDs), recent studies of Josephson plasma resonance (JPR) have been carried out in Bi-2212.[11,12] They suggest the occurrence of two distinct liquid phases above the irreversibility line, with stronger and weaker c-axis correlations of pancake vortices, in agreement with a recent theoretical study.[13] Note, however, that the analysis of JPR experiments is still the subject of intense debate.[14]

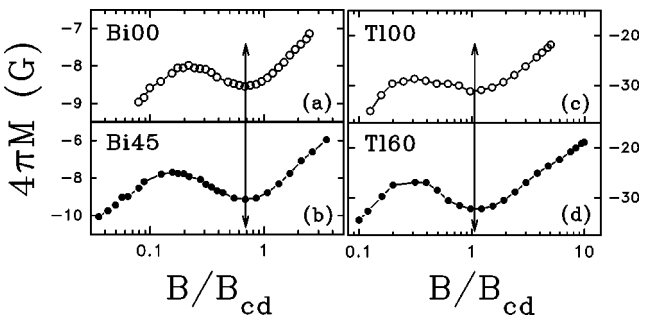

FIG. 3. Reversible magnetization curves versus B/B_{cd} (see text): (a) at $T=70$ K, for $\theta_i=0°$ in Bi-2212, (b) at $T=70$ K, for $\theta_i=45°$ in Bi-2212, (c) at $T=80$ K, for $\theta_i=0°$ in Tl-2212, (d) at $T=80$ K, for $\theta_i=60°$ in Tl-2212. The arrows emphasize the close relationship between B_{cd} and the location of the dip.

For the present study, the key point is that reversible magnetization can be related to the behavior of pancake vortices, for which the pinning energy depends on the track projections on the ab planes. Since the track inclination modifies the size of these projections, one may expect a variation in the effective pinning energy.

IV. PINNING ENERGY VERSUS EFFECTIVE DEFECT SIZE

A. Experimental precautions

The most direct way[2,3] to extract the pinning energy involves measurements of reversible magnetization in the unirradiated state, denoted hereafter $M_{\rm un}$. Therefore, $M_{\rm rev}$ has been investigated, before and after irradiation, in the two samples chosen for this study (Tl00 and Tl60). The measurements of $M_{\rm un}$ also allow us to correct the unavoidable uncertainty about the volumes, by assuming that $M_{\rm un}(B,T/T_c)$ is the same in both samples. In practice, the smallest volume was corrected by a multiplicative factor ensuring the superimposition of the $[\partial M_{\rm un}/\partial\ln B](T/T_c)$ curves in both samples.

B. Basic equations

The reversible magnetization $M_{\rm rev}$ can be derived from the free energy F, through the relation

$$M_{\rm rev}=-\frac{\partial}{\partial B}\left[F-\frac{B^2}{8\pi}\right]. \tag{4.1}$$

In the frame of a London approach,[1] F can be written as

$$F\simeq\frac{B^2}{8\pi}+n\varepsilon_l-n_p\Delta\varepsilon, \tag{4.2}$$

where n_p is the areal density of vortices localized onto tracks, while n is the total areal density of vortices, ε_l and ε_p are the line energies of a vortex located outside of the tracks or in one of them, respectively, $\Delta\varepsilon=\varepsilon_l-\varepsilon_p$, is the pinning energy per unit length, ε_0 is the basic energy scale: $\varepsilon_0=(\Phi_0/4\pi\lambda_{ab})^2$, where λ_{ab} is the in-plane penetration depth, and d is the mean vortex spacing, connected to B by the relation: $B=n\times\Phi_0\simeq\Phi_0/d^2$.

The free energy in the virgin state $F_{\rm un}$ can be estimated from Eq. (4.2) by considering $n_p=0$, and by using the complete expression of ε_l including the core contribution $\varepsilon_l=\varepsilon_0[\ln(\lambda_{ab}/\xi_{ab})+\frac{1}{2}]$, where ξ_{ab} is the in-plane coherence length ($B_{c2}=\Phi_0/2\pi\xi_{ab}^2$). In this way, one obtains

$$F_{\rm un} \simeq \frac{B^2}{8\pi} + \frac{B\varepsilon_0}{\Phi_0}\left[\ln\left(\frac{d}{\xi_{ab}}\right) + \frac{1}{2}\right]. \tag{4.3}$$

Except for a factor close to unity ($\eta' \simeq 0.381$), which absorbs numerical constants, this is the standard expression of the modified London model, when one roughly takes into account the core contribution[15,16]

$$F_{\rm un} = \frac{B^2}{8\pi} + \frac{B\varepsilon_0}{\Phi_0}\left[\ln\sqrt{\frac{\eta' B_{c2}}{B}} + \frac{1}{2}\right]. \tag{4.4}$$

From Eq. (4.1), one derives

$$M_{\rm un} = -\frac{\varepsilon_0}{2\Phi_0}\ln\left(\frac{\eta' B_{c2}}{B}\right). \tag{4.5}$$

Note the absence of a factor $e \simeq 2.72$, in the denominator, compared to the pure London model. It turns out that this factor is cancelled out by the core term in $F_{\rm un}$. This core contribution makes Eq. (4.5) closer to the Hao-Clem model[17] than the pure London approach. Combining Eqs. (4.1) and (4.2), the reversible magnetization in the irradiated state can be expressed as

$$M_{\rm ir} = M_{\rm un} + \Delta\varepsilon \times \left(\frac{\partial n_p}{\partial B}\right). \tag{4.6}$$

C. Analysis of the low field regime

Following the literature,[2,3] one considers that all the vortices are pinned on tracks in the low field regime ($B \ll B_{cd}$), i.e., $n_p = n$. As a consequence, $(\partial n_p/\partial B) = 1/\Phi_0$, and $\Delta\varepsilon$ can be directly derived from the shift in magnetization $\Delta M = M_{\rm ir} - M_{\rm un}$:

$$\Delta\varepsilon = \Delta M \times \Phi_0. \tag{4.7}$$

Some examples of $M_{\rm rev}$-vs-ln(B) curves, before and after irradiation, are given in Fig. 4. One observes that $M_{\rm ir}$ is shifted from $M_{\rm un}$, even in the high field range for which $B \gg B_{cd}$. This behavior was systematically observed, for all T values, not only in Tl00 and Tl60, but also in another pair of Tl-2212 crystals irradiated in the same conditions. Similar results have also been obtained in Refs. 1 and 2. By contrast, in Ref. 10, the curves merge together at high fields, and $|M_{\rm ir}|$ is found to be larger than $|M_{\rm un}|$ in the region of the dip. This last behavior seems inconsistent with Eq. (4.6) since negative values of $\Delta\varepsilon \times (\partial n_p/\partial B)$ are not expected. In our case, the persistence of a clear shift between $M_{\rm ir}$ and $M_{\rm un}$, for $B \gg B_{cd}$, questions the reliability of $M_{\rm un}$ in Eq. (4.6). In fact, the ''virgin magnetization'' involved in Eq. (4.6) is related to the contribution of vortices located outside the tracks. Therefore, an extrapolation of $M_{\rm ir}(B \gg B_{cd})$ down to low fields should be more relevant to the present analysis than $M_{\rm un}$ measured before irradiation.

This procedure actually permits us to take into account irradiation induced modifications of superconducting parameters, which affect all the vortices even those outside of the tracks. The two main expected effects are a slight decrease of T_c (found to be about 2 K, for Tl00 and Tl60), and an increase of λ_{ab}. The latter effect has been previously addressed[1,18] by considering the influence of tracks on magnetic screening. This approach leads to renormalize the λ_{ab} value of the virgin state to an effective, larger penetration depth $\tilde{\lambda}_{ab}$:

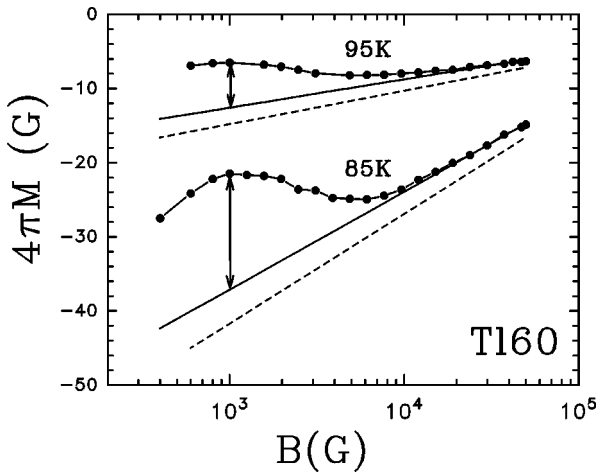

FIG. 4. Reversible magnetization curves versus field, illustrating the extraction of the pinning energy at $B = 1000$ G (sample Tl60). The dashed lines are logarithmic fits to the data obtained before irradiation, while the filled circles are the measurements after irradiation. The solid, straight lines are the corrected ''virgin curves,'' leading to a superimposition on the ''irradiated ones'' in the high field regime (see text). The arrows display the chosen criterion for ΔM (see text).

$$\tilde{\lambda}_{ab}^2 = \lambda_{ab}^2/(1 - 2\pi R_{ab}^2 n_{cd}), \tag{4.8}$$

where n_{cd} and R_{ab} are the areal density and the characteristic size of the defects in the ab planes, respectively. For tracks parallel to c, one has $R_{ab} = R$, while for tracks at θ_i relative to c, we consider[19] $R_{ab} \approx \sqrt{R \times R/\cos\theta_i}$. With $R \simeq 5$ nm and $n_{cd} \simeq 5 \times 10^{10}$ cm^{-2}, one obtains $(1 - 2\pi R_{ab}^2 n_{cd}) \simeq 0.92$. This value is independent of θ_i, since the increase of R_{ab}^2 (by $1/\cos\theta_i$) just counterbalances the decrease of n_{cd} (by $\cos\theta_i$). The modification of λ_{ab} induces a renormalization of ε_0 and $M_{\rm un}$:

$$\widetilde{\varepsilon_0} = \varepsilon_0(1 - 2\pi R_{ab}^2 n_{cd}), \tag{4.9a}$$

$$\widetilde{M_{\rm un}} = M_{\rm un}(1 - 2\pi R_{ab}^2 n_{cd}). \tag{4.9b}$$

It turns out that this correction directly yields $\widetilde{M_{\rm un}}(\ln B)$ curves which are very close to $M_{\rm ir}(\ln B)$ at high fields, i.e., well consistent with a regime where most of the vortices are outside the tracks. This behavior prompted us to make use of $\widetilde{M_{\rm un}}$, instead of $M_{\rm un}$, for the derivation of ΔM and $\Delta\varepsilon$. In practice, we adjusted, in each case, the parameter $K = \widetilde{M_{\rm un}}/M_{\rm un}$, leading to a merging of $\widetilde{M_{\rm un}}(\ln B)$ with $M_{\rm ir}(\ln B)$ at high fields. Owing to the reduction of T_c after irradiation, the K values slightly decrease as T increases, but they stay in the range 0.93–0.85, consistently with the estimate of $(1 - 2\pi R_{ab}^2 n_{cd})$.

The derivation of $\Delta\varepsilon$ from Eq. (4.7) can be performed only for fields much lower than B_{cd}. The data led us to choose $B = 1000$ G, in order to allow for a determination of $\Delta\varepsilon$ on a broad enough temperature range, in both samples.

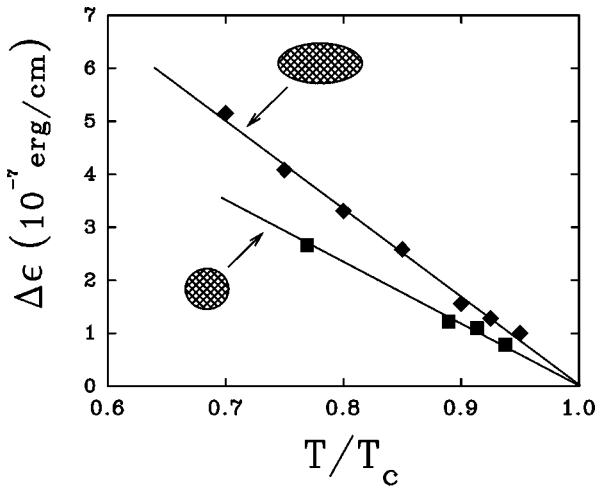

FIG. 5. Pinning energy versus reduced temperature, at $B=1000$ G, in Tl00 (filled squares) and Tl60 (filled diamonds). The track projections on the ab planes, in Tl00 and Tl60, are sketched by the circle and the ellipse, respectively. The solid lines are linear fits to the data (see text).

D. Results

Figure 5 shows $\Delta\varepsilon$ versus $t=T/T_c$, for Tl00 and Tl60, at $B=1000$ G. These values were obtained from $\Delta M=M_{\rm ir}-\widetilde{M_{\rm un}}$, but the results are qualitatively identical for $\Delta M=M_{\rm ir}-M_{\rm un}$ [the $\Delta\varepsilon(t)$'s are just slightly shifted to higher values in the latter case]. In any cases, the $\Delta\varepsilon$ values are found to be larger for $\theta_i\neq 0°$ than for $\theta_i=0°$. In the available temperature range ($t\geqslant 0.7$), one finds a good linear dependence $\Delta\varepsilon=A^*(1-t)$, as in Refs. 2 and 3. The prefactors are found to be $A({\rm Tl00})\simeq 11.7\times 10^{-7}$erg/cm and $A(Tl60)\simeq 16.7\times 10^{-7}$ erg/cm. These values are of the same order of magnitude than those of Refs. 2 and 3. It is convenient to express $\Delta\varepsilon$ as a function of the basic energy scale ε_0. The $\varepsilon_0(t)$ values were derived from Eq. (4.5), using the data before irradiation. The analysis of the whole temperature range is well consistent with a BCS-like dependence, yielding $\lambda_{ab}({\rm nm})\simeq 190/\sqrt{1-t^2}$. However, if one just considers the high-T range corresponding to the study after irradiation ($t\geqslant 0.7$), ε_0 exhibits a linear dependence: $\varepsilon_0({\rm erg/cm})=12.3\times 10^{-7}(1-t)$. Since the $\Delta\varepsilon$ values in Fig. 5 were derived from the renormalized magnetization $\widetilde{M_{\rm un}}$ the most relevant energy scale is $\widetilde{\varepsilon_0}\simeq 0.92\times\varepsilon_0$. The pinning energies for Tl00 and Tl60 can finally be rewritten as

$$\Delta\varepsilon({\rm Tl00})\simeq 1.03\widetilde{\varepsilon_0}, \tag{4.10a}$$

$$\Delta\varepsilon({\rm Tl60})\simeq 1.48\widetilde{\varepsilon_0}. \tag{4.10b}$$

E. Discussion

The two main features of these results are (i) $\Delta\varepsilon$ values close to $\widetilde{\varepsilon_0}$, (ii) existence of a slight increase of $\Delta\varepsilon$ with R_{ab} (characteristic size of the track projection on the ab planes). These features are in accordance with the theoretical expressions[20–22] of $\Delta\varepsilon$ (replacing ε_0 by $\widetilde{\varepsilon_0}$)

$$\Delta\varepsilon=\frac{\widetilde{\varepsilon_0}}{2}\left[1+\ln\left(\frac{R_{ab}}{\sqrt{2}\xi_{ab}}\right)^2\right]\quad\text{for}\quad R_{ab}\geqslant\sqrt{2}\xi_{ab}, \tag{4.11a}$$

$$\Delta\varepsilon=\frac{\widetilde{\varepsilon_0}}{2}\left(\frac{R_{ab}}{\sqrt{2}\xi_{ab}}\right)^2\quad\text{for}\quad R_{ab}\leqslant\sqrt{2}\xi_{ab}. \tag{4.11b}$$

It turns out that Eq. (4.11a) is the most consistent with our data. Indeed, the experimental $\Delta\varepsilon$ values are larger than $\widetilde{\varepsilon_0}/2$, and their T dependence appears to be essentially related to $\widetilde{\varepsilon_0}(t)$.

Let us try to quantify the expected influence of the track inclination on $\Delta\varepsilon$. Since $R_{ab}=R$ for Tl00, Eqs. (4.10a) and (4.11a) lead to $\ln(R/\sqrt{2}\xi_{ab})\simeq 0.5$. According to a previous study[7] on Tl-2212, one can consider an average value $\xi_{ab}\simeq 3$ nm in the T range of Fig. 5. This yields a R value around 7 nm, i.e., slightly larger than the amorphous core itself ($\simeq 5$ nm). It is not unexpected to find a value of the effective pinning radius which is larger than the amorphous core,[2] since it is clear that superconductivity must be affected in the matrix just surrounding heavy-ion tracks. For Tl60, one has $R_{ab}\approx\sqrt{2}R$. Using the above estimates of R and ξ_{ab}, Eq. (4.11a) yields $\Delta\varepsilon\approx 1.35\widetilde{\varepsilon_0}$ for Tl60, which is close to the experimental result [Eq. (4.10b)]. Beyond this rather good quantitative agreement, the important point is that a measurable difference in $\Delta\varepsilon$ could be expected between $\theta_i=0°$ and $\theta_i=60°$, and such a difference has been actually observed.

V. MODELIZATION OF THE FIELD DEPENDENT SHIFT OF $M_{\rm rev}$ BETWEEN THE VIRGIN AND IRRADIATED STATES

A. Preliminary remarks

The first attempt to account for the shape of $M_{\rm ir}$-vs-ln(B) curves in the whole field range, i.e., from $B\ll B_{cd}$ up to $B\gg B_{cd}$, was carried out by Bulaevskii, Vinokur, and Maley (BVM model[5]). This model assumes completly decoupled pancakes and includes entropy contribution to the free energy. The pancakes are distributed among two types of site, corresponding to a localization in one of the tracks or between them. This problem can be mapped onto the statistics of fermions. The general expression of $M_{\rm ir}(\ln B)$ derived from this model was shown to reasonably fit to the data of Refs. 2 and 3. We propose here another approach based on Ref. 1, which included the random nature of the track distribution. The entropy is not taken into account in this case, thus the general expression of $M_{\rm ir}$ is just given by Eq. (4.6).

B. Modelization

The problem is to determine the *accommodation function* $n_p(n)$. The required limit behaviors—already assumed in Sec. IV—are $n_p\simeq n$ for $n\ll n_{cd}$, and $n_p\simeq n_{cd}$ for $n\gg n_{cd}$. We presently need to construct a continuous function over the whole range of n/n_{cd}. To do this, it must be realized that the vortex-vortex interactions oppose a complete accommodation of the vortices to the random track distribution.

In the simplest quantitative approach,[1] one estimates the shortest distance ρ separating two pinned vortices. The repulsive energy per unit length between two vortices, sepa-

rated by the mean vortex spacing d, is equal[15] to $2\varepsilon_0 \ln(\lambda_{ab}/d)$. One can derive ρ by balancing the pinning and interaction energies, when one vortex approachs the other to fill a track. The distance ρ corresponds to the situation where the energy decrease due to pinning of the second vortex just equals the increase of interaction energy. One obtains $\rho = d \times \exp(-\Delta\varepsilon/2\varepsilon_0)$. For very weak pinning ($\Delta\varepsilon \ll \varepsilon_0$), one has $\rho \sim d$ (the vortex lattice is almost undisturbed), while for strong pinning, ρ tends to 0. It may be more useful to consider the distance $\Lambda = d - \rho$, which corresponds to the largest possible displacement of a vortex from its equilibrium position in a lattice. Gray *et al.*[23] have precisely evaluated this quantity by considering the interaction with the neighboring vortices over a large scale. Within this approach,

$$\Lambda = \sigma d, \tag{5.1a}$$

$$\sigma = \beta \sqrt{\frac{\Delta\varepsilon}{2\varepsilon_0}}, \tag{5.1b}$$

with $\beta \sim 0.77$. This is a more general result than the previous approach [$\sigma = 1 - \exp(-\Delta\varepsilon/2\varepsilon_0)$], which just involves two vortices. This previous result actually corresponds to the case of a large vortex displacement along a nearest-neighbor direction. According to Ref. 23, this specific situation leads to a slightly different parameter $\beta \sim 0.62$. With this value, it turns out that both expressions of σ are nearly superimposed as long as $\Delta\varepsilon/2\varepsilon_0 < 2$.

In Ref. 1, n_p is estimated by considering that cells of size ρ (in a closely packed arrangement) cannot contain more than one pinned vortex. This yields an upper limit for n_p, which can be considered as a good approximation for $B > B_{cd}$. Nevertheless, this expression obviously fails for $B < B_{cd}$, since it can exceed n. In order to describe the whole field range, we use a slightly different approach, with cells of size Λ, centered on the positions of vortices in a lattice (see inset of Fig. 6). To simplify, we considered a square lattice and square cells. Note that the cells do not overlap, even for the largest value of σ. A vortex is pinned if its cell contains at least one track. This approach ensures that the distance between two pinned vortices is always larger than ρ, but it can lead to underestimate n_p. For instance, when $B \gg B_{cd}$, this model does not take into account the possibility of local distortions in the vortex lattice, allowing for the occupancy of tracks located outside all of the cells. Bearing in mind the limits of this approach, we derive an *approximation* of n_p, by multiplying n by the probability for finding at least one track in a cell of size Λ. This probability is $1 - P_0$, where P_0 is the probability for finding no track in the cell. According to the Poisson distribution of the tracks $P_0 = \exp(-\alpha)$, where α is the mean number of tracks per cell ($\alpha = \Lambda^2 n_{cd} = \sigma^2 n_{cd}/n$). It results that

$$n_p = n[1 - \exp(-\sigma^2 n_{cd}/n)], \tag{5.2}$$

σ is the pinning parameter [Eq. (5.1)], which increases from 0 without pinning, up to 1 for maximal pinning. The function n_p/n_{cd} versus n/n_{cd} is shown in Fig. 6, for a typical value of σ. The reversible magnetization can be directly derived from Eqs. (4.6) and (5.2). Including also the renormalization of λ_{ab} [Eq. (4.9b)], one obtains

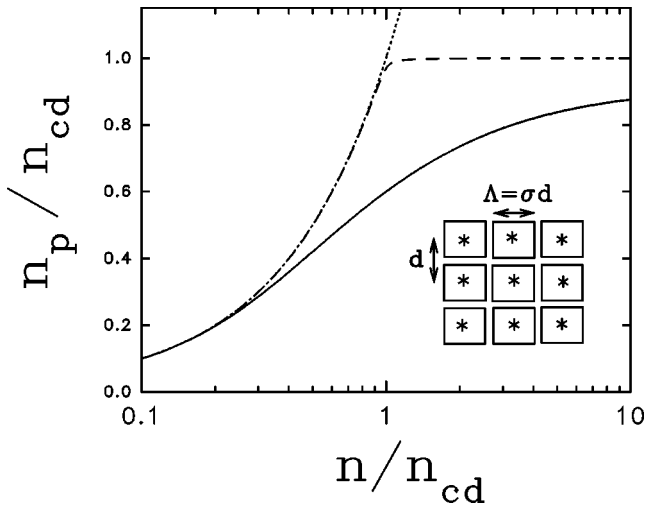

FIG. 6. Calculated densities of trapped pancake vortices (n_p) as function of the total vortex density per ab planes (n) present work with $\sigma = 0.92$ (solid line), BVM model[5] with $p = 1000$ (dashed line). The low field limit of complete pinning ($n = n_p$) corresponds to the dotted line, and n_{cd} is the track density in each ab plane. The present modelization involves an array of cells (size $\Lambda = \sigma d$), centered on the equilibrium vortex positions (stars), and separated by the distance d (see text).

$$M_{\rm ir} = M_{\rm un}(1 - 2\pi R_{ab}^2 n_{cd}) + \frac{\Delta\varepsilon}{\Phi_0}[1 - \exp(-\alpha) - \alpha\exp(-\alpha)], \tag{5.3}$$

with $\alpha = \sigma^2 n_{cd}/n$.

C. Comparison to the data

Figure 7 shows examples of fits to experimental $M_{\rm ir}$-vs-ln(B) curves via Eq. (5.3). We used Tl60 for which the reversible domain is the largest in field and temperature. As previously discussed, the first term in the right-hand side

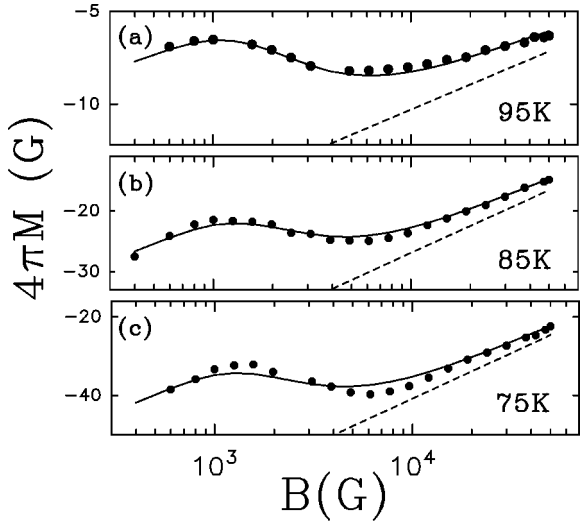

FIG. 7. Data of reversible magnetization versus field in Tl60 (filled circles), together with fits to Eq. (5.3) (solid lines) and curves before irradiation (dashed lines), at (a) $T = 95$ K, (b) $T = 85$ K, and (c) $T = 75$ K.

of Eq. (5.3) was derived from an extrapolation of the high field range. The parameter B_{cd} was fixed to its nominal value, i.e., $B_{cd}=5000$ G for Tl60. The fits yield values of the parameter σ^2, which is related to the shape of the crossover between the low and high field regimes. In the whole T range, it was found that $\sigma^2=0.92\pm0.05$. This parameter is linked to $\Delta\varepsilon$ by Eq. (5.1b), which can be rewritten as $\sigma^2=\beta^2(\Delta\varepsilon/2\widetilde{\varepsilon_0})$, where ε_0 has been substituted by $\widetilde{\varepsilon_0}$. With the $\Delta\varepsilon$ values found in Sec. IV [Eq. (4.10)] and $\beta\sim0.77$, the expected σ^2 value should be equal to 0.44, i.e., smaller than half the experimental value. Nevertheless, it was pointed out in Ref. 23 that the calculated σ^2 value is increased by factors $\sim2-3$ when one considers a highly disordered vortex array, as it must be the case around B_{cd}. Considering this correction, the experimental values of $\Delta\varepsilon$ and σ^2 become consistent with each other. Note, however, that one must be cautious in the quantitative comparison between $\Delta\varepsilon$ and σ^2. Indeed, $\Delta\varepsilon$ is rather well defined by the height of the ''jump'' between the low and high field regimes, whereas the fitting yields a large *apparent* σ^2 value, to counterbalance the weakness of the model which ''oversmooths'' the $n_p(n)$ variation. As a matter of fact, Fig. 7 shows that the experimental dip in $M_{\rm ir}(\ln B)$ is more pronounced than in the fitting curves. The agreement is better as T increases, i.e., as the effective pinning energy decreases.

D. Comparison to the BVM model

Let us now compare our fits with those derived from the BVM model.[5] Following the proposed method, the expression used to fit to the data is

$$M_{\rm ir}=\widetilde{M}_{\rm ir}+\frac{kT}{s\Phi_0}\ln\left(\frac{u+\sqrt{u^2+pb}}{1+p}\right), \tag{5.4}$$

$$u=[1+(1-b)p]/2,$$

$$b=B/B_{cd},$$

$$p=(2kT/\varepsilon_0 s)(B_{cd}/B_{c2})\exp(s\Delta\varepsilon/kT),$$

where $\widetilde{M}_{\rm ir}$ is the linear extrapolation of $M_{\rm ir}$-vs-ln(B), from the low field regime ($B\ll B_{cd}$) to higher fields, the interlayer spacing s was fixed to 1.5 nm, B_{cd} was fixed to 5000 G, corresponding to $B_{\Phi t}=1$ T with $\theta_i=60°$, according to a previous study,[7] we took B_{c2} (T)$=180\times(1-t)$, and ε_0 was substituted by $\widetilde{\varepsilon_0}$.

The fitting yields p values which rapidly decrease as T increases, e.g., $p\simeq1000$, 150, and 1.5 for $T=75$, 85, and 95 K, respectively. These values are in good agreement with those derived[5] from the data of Refs. 2 and 3.

Figure 8 displays, at a given temperature, the fitting curves from Eqs. (5.3) and (5.4). Comparing to the data, the crossover around B_{cd} is clearly too smooth in our model, while it is too steep in the BVM model. This must be related to the fact that our model underestimates n_p, whereas it is likely overestimated in Ref. 5, since the spatially-random track distribution is not taken into account. Recently,[24] it was also suggested that the shape of $M_{\rm rev}$-vs-ln(B) could be affected by a coupling transition of the pancakes as field is increased. The fitting quality of our model increases with T (see Fig. 7), whereas the BVM model is better as T decreases. The difference between the two models is emphasized in Fig. 6, through the calculated field dependence of n_p in both cases, with parameters corresponding to the fitting curves of Fig. 8.

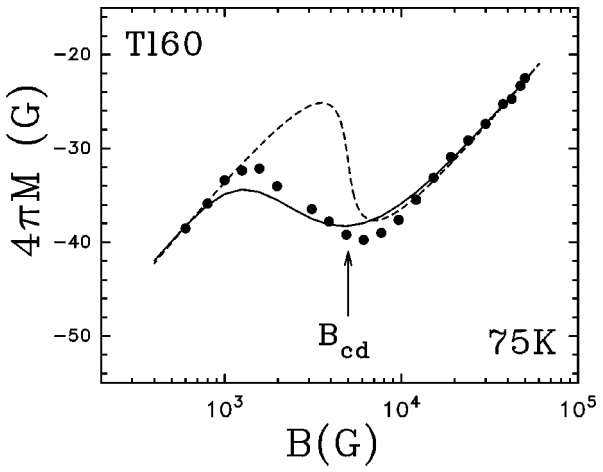

FIG. 8. Field dependence of the reversible magnetization of Tl60 at 75 K (filled circles), together with the fitting curves to Eq. (5.3) (present work, solid line) and Eq. (5.4) (BVM model, [5] dashed line).

VI. CONCLUSION

Reversible magnetization has been investigated, as function of field applied along c, in Tl-2212 and Bi-2212 single crystals containing columnar defects (CDs) either parallel to the c axis, or tilted by an angle θ_i. In all cases, the $M_{\rm rev}$-vs-ln(B) curves exhibit the same unusual shape, with a field region of negative slope smoothly connecting two nearly parallel lines of positive slope, in the low and high field regimes. These features, previously reported for $\theta_i=0$, are thus found to persist for highly ''misaligned'' situations, i.e., for large angles (e.g., 60°) between the field and the CDs. Moreover, comparisons between $\theta_i=0°$ and $\theta_i\neq0°$ clearly indicate that the dip in the crossover region takes place for the same ratio B/B_{cd}, where B_{cd} is the field at which the vortex and track densities, per ab plane, are the same.

For a few samples, reversible magnetization curves were recorded before and after irradiation. These measurements clearly display the persistence of a shift in the high field regime ($B\gg B_{cd}$) between the curves of the virgin and unirradiated states. Note that this behavior is still controversial in the literature.[1–3,10] In the present study, the shift was systematically observed in four samples measured before and after irradiation. It is shown that such a decrease of the $|M|$ values after irradiation, in the high field regime, can be accounted for by an increase of the effective penetration depth due to a screening effect by the tracks.

The pinning energy, $\Delta\varepsilon$, has been determined in Tl-2212 crystals irradiated at $\theta_i=0°$ or $\theta_i=60°$. The pinning energy was found to be slightly larger in the latter case, namely (in erg/cm, for $t\geqslant0.7$), $\Delta\varepsilon(0°)\simeq11.7\times10^{-7}(1-t)$ and $\Delta\varepsilon(60°)\simeq16.7\times10^{-7}(1-t)$. This variation is in good agreement with the expected increase of $\Delta\varepsilon$ with the size of

the track projections on the ab planes, which is the relevant parameter to pancake pinning. This result also reinforces the interpretation recently proposed to account for the existence of larger critical current densities with $\theta_i = 75°$ than with $\theta_i = 0°$, at low field in Bi-2212.[25]

A model was proposed to account for the smooth character of the crossover between the low field ($B \ll B_{cd}$) and high field regimes ($B \gg B_{cd}$). We tried to estimate how the vortex localization is affected by the random nature of the track distribution. Despite the roughness of some assumptions, the fitting curves derived from this approach are in reasonable agreement with the data. However, this model omits the influence of entropy contribution to the free energy.[5] A next step would consist in combining such entropic effects with those induced by the spatially random track distribution.

ACKNOWLEDGMENTS

The authors thank C. Martin (CRISMAT, Caen) for providing us with high quality Tl-2212 single crystals and C. Poirier (ISMRA, Caen) for technical assistance in making the sample holders. We are also grateful to the staff of CIRIL (Caen) for their support during the heavy-ion irradiations, and to A. Buzdin (CPTM, Bordeaux) for many useful discussions.

[1] A. Wahl, V. Hardy, J. Provost, Ch. Simon, and A. Buzdin, Physica C **250**, 163 (1995).
[2] Q. Li, Y. Fukumoto, Y. Zhu, M. Suenaga, T. Kaneko, K. Sato, and Ch. Simon, Phys. Rev. B **54**, R788 (1996).
[3] C. J. van der Beek, M. Konczykowski, T. W. Li, P. H. Kes, and W. Benoit, Phys. Rev. B **54**, R792 (1996).
[4] V. Hardy, A. Wahl, S. Hébert, A. Ruyter, J. Provost, D. Groult, and Ch. Simon, Phys. Rev. B **54**, 656 (1996).
[5] L. N. Bulaevskii, V. M. Vinokur, and M. P. Maley, Phys. Rev. Lett. **77**, 936 (1996).
[6] A. Ruyter, Ch. Simon, V. Hardy, M. Hervieu, and A. Maignan, Physica C **225**, 235 (1994).
[7] A. Wahl, A. Maignan, C. Martin, V. Hardy, J. Provost, and Ch. Simon, Phys. Rev. B **51**, 9123 (1995).
[8] V. Hardy, A. Ruyter, J. Provost, D. Groult, and Ch. Simon, Physica C **224**, 143 (1994).
[9] A. Wahl, M. Hervieu, G. van Tendeloo, V. Hardy, J. Provost, D. Groult, Ch. Simon, and B. Raveau, Radiat. Eff. Defects Solids **133**, 293 (1995).
[10] C. J. van der Beek, M. Konczykowski, T. W. Li, and P. H. Kes, Physica C **282-287**, 2101 (1997).
[11] M. Sato, T. Shibauchi, S. Ooi, T. Tamegai, and M. Konczykowski, Phys. Rev. Lett. **79**, 3759 (1997).
[12] M. Kosugi, Y. Matsuda, M. B. Gaifullin, L. N. Bulaevskii, N. Chikumoto, M. Konczykowski, J. Shimoyama, K. Kishio, K. Hirata, and K. Kumagai, Phys. Rev. Lett. **79**, 3763 (1997).
[13] L. N. Bulaevskii, M. P. Maley, V. M. Vinokur, Phys. Rev. B **57**, R5626 (1998).
[14] E. B. Sonin, Phys. Rev. Lett. **79**, 3732 (1997).
[15] P. G. de Gennes, *Superconductivity of Metals and Alloys* (W. A. Benjamin, New York, 1966).
[16] V. G. Kogan, A. Gurevich, J. H. Cho, D. C. Johnston, M. Xu, J. R. Thompson, and A. Martynovich, Phys. Rev. B **54**, 12 386 (1996).
[17] Z. Hao, J. R. Clem, Phys. Rev. Lett. **67**, 2371 (1991).
[18] A. Buzdin and D. Feinberg, Physica C **256**, 303 (1996).
[19] In a recent study, A. Buzdin and M. Daumens [Physica C **294**, 257 (1998)] have shown that R_{ab} should rather be given by the relation $R_{ab} \simeq [R + (R/\cos\theta_i)]/2$. It turns out that both formulas yield very close results for moderate geometrical anisotropy. For $\theta_i = 60°$, we consider $R_{ab} \simeq \sqrt{2}R$, while the formula of Buzdin *et al.* leads to $R_{ab} \simeq (3/2)R$.
[20] G. S. Mkrtchyan and V. V. Shmidt, Sov. Phys. JETP **34**, 195 (1972).
[21] D. R. Nelson and V. M. Vinokur, Phys. Rev. B **48**, 13 060 (1993).
[22] G. Blatter, M. V. Feigel'man, V. B. Geshkenbein, A. I. Larkin, and V. M. Vinokur, Rev. Mod. Phys. **66**, 1125 (1994).
[23] K. E. Gray, D. G. Steel, J. D. Hettinger, and M. Eddy, Phys. Rev. B **57**, 13 894 (1998).
[24] N. Chikumoto, M. Kosugi, Y. Matsuda, M. Konczykowski, and K. Kishio, Phys. Rev. B **57**, 14 507 (1998).
[25] S. Hébert, V. Hardy, G. Villard, M. Hervieu, Ch. Simon, and J. Provost, Physica C **299**, 259 (1998).